molecular pharmaceutics

articles

Molecular Dynamics Simulations of Functional Group Effects on Solvation Thermodynamics of Model Solutes in Decane and Tricaprylin

Sagar S. Rane and Bradley D. Anderson*

Department of Pharmaceutical Sciences, College of Pharmacy, University of Kentucky, Lexington, Kentucky 40536

Received June 3, 2008; Revised Manuscript Received August 16, 2008; Accepted September 2, 2008

Abstract: Triglycerides and related fatty acid esters constitute a large percentage of the lipid excipients employed in the development of lipid-based drug formulations. Computer simulations can provide useful information on the structural, dynamic, and thermodynamic properties of these systems and may ultimately be valuable in predicting relative drug solubilities in lipid vehicles. This study utilized all-atom molecular dynamics simulations to explore the solvation of several model solutes in lipid vehicles. First, a combined thermodynamic perturbation and integration approach was employed to calculate functional group contributions to the free energy of transfer from *n*-decane to tricaprylin for a set of polar substituents attached to the 9-position of anthracene. A scaling factor of 0.79 for all atomic charges in the dry lipid (where the unscaled charges were obtained at the level of the HF/6-31G* basis set) was necessary in order to match the calculated group contributions to the free energies of transfer with their experimental values at 37 °C. A second set of simulations was performed in water-saturated tricaprylin containing a single molecule of benzamide to explore the state of organization of solvent molecules, the distribution of water molecules, and the local environment surrounding the solute. Radial distribution functions revealed evidence of local structure in the liquid triglyceride. The dissolved water was found to exist ~50% as monomers and 50% as self-associated species. Substantial hydrogen-bonding of benzamide with ester carbonyl oxygen atoms was observed.

Keywords: Triglycerides; molecular dynamics simulations; thermodynamic perturbation and integration; transfer free energies; functional group effects; structure

Introduction

Lipid-based formulations are generally regarded as a promising route for solubilization of highly lipophilic drugs to increase oral bioavailability and possibly reduce food effects.[1] Despite these potential advantages, the commercialization of lipid-based formulations for such compounds has been limited due to numerous factors, including high materials costs, manufacturing and scale-up difficulties, chemical factors such as toxicity, and physical factors such as the lack of knowledge of phase behavior and structure−property relationships in these systems. Computer simulations may contribute to a better understanding of structure−property relationships and other physical properties of lipid formulations because they can provide information at a molecular level and allow the investigator to explore a wide variety of lipid-based systems.

Typically, a lipid-based formulation employs at least three components, namely, oil, surfactant, and water.[2] Other excipients, such as cosurfactants and water soluble cosol-

* To whom correspondence should be addressed. Mailing address: A323A, ASTeCC Building, University of Kentucky, Lexington, KY 40506. E-mail: bande2@email.uky.edu. Telephone: 859-218-6536. Fax: 859-257-2489.

(1) Araya, H.; Nagao, S.; Tomita, M.; Hayashi, M. The novel formulation design of self-emulsifying drug delivery systems (SEDDS) type o/w microemulsion I: Enhancing effects on oral bioavailability of poorly water soluble compounds in rats and beagle dogs. *Drug Metab. Pharmacokinet.* **2005**, *20*, 244–256.

(2) Strickley, R. G. Solubilizing excipients in oral and injectable formulations. *Pharm. Res.* **2004**, *21*, 201–230.

10.1021/mp8000606 CCC: $40.75
Published on Web 11/06/2008

vents, may also be present. A computational method to reliably estimate relative solubilities in various lipid-based vehicles would be quite useful in guiding the selection of the appropriate delivery system for a given drug. Recently, the authors determined solubilities of several model solutes in triglyceride/monoglyceride/water mixtures in the "w/o microemulsion" region[3] at 37 °C and presented a thermodynamic model designed to understand and predict relative solubilities based on structure-based descriptors of the solute and the solvent. In this paper, computer simulations in a model triglyceride or in a reference hydrocarbon solvent were conducted to gain a better understanding of local solvent organization and solvation thermodynamics of several model solutes for which experimental solubility data were available. A thermodynamic perturbation and integration approach was adopted to calculate the contributions of various functional groups to the free energies of transfer of a set of anthracene analogues between two model lipids, tricaprylin and *n*-decane.

While molecular dynamics simulations of lipid systems have been frequently reported in the literature, most have focused on the lipid bilayer and its structural features or transport properties.[4−7] Recently, Warren et al. employed molecular dynamics simulations to study the spontaneous aggregation of bile salts in an aqueous environment to form micellar structures,[8] but only a few simulations have been conducted to investigate the properties of pure lipids (triglycerides and derivatives) and lipid mixtures. Chandrasekhar and van Gunsteren investigated the structure of the gel or α-phase of trioctanoin and found that the size of the ester carbon plays a significant role in determining the mean square area per chain in triglycerides.[9] Sum et al. recently proposed a new molecular model to predict the thermodynamic and transport properties of triacylglycerols.[10] Their results showed that, in the liquid phase, triglycerides self-assemble to form layered structures comparable to the structure found in their crystalline state. They found that the alignment of the polar groups in triglycerides leads to the formation of structures resembling bilayers. Structure−property relationships in triglycerides were investigated by changing the stiffness of the three fatty acid chains. The authors[10] also found that it is imperative to properly account for the structural details of triglycerides in order to accurately calculate sensitive dynamic properties such as the viscosity. Other independent studies such as X-ray scattering experiments conducted on liquid triglycerides[11,12] slightly above their melting points have also revealed that liquid triglycerides retain small domains of double layer or bilayer structure (similar to their crystalline form). The only disparity is that the fatty acid side chains are melted (i.e., disordered). Engelsen et al. employed molecular dynamics simulations to study the interaction of trilaurin with water and the dynamics of triglyceride folding in an aqueous solution.[13] van Buuren et al. studied the diglyceride−water interface and discovered that the addition of cosurfactants such as monoglycerides and fatty acids to the oil phase lowered the surface tension and increased the total order of all molecules at the interface.[14] On the other hand, a number of molecular dynamics simulations of pure hydrocarbons such as decane have been reported. These studies have successfully investigated dynamic properties such as diffusion coefficients and viscosity as well as thermodynamic properties such as adsorption behavior.[15−18] The force fields and methods currently employed in simulations seem to have been satisfactory for calculating properties of short chain *n*-alkanes.

(3) Rane, S. S.; Cao, Y.; Anderson, B. D. Quantitative solubility relationships and the effect of water uptake in triglyceride/monoglyceride microemulsions. *Pharm. Res.* **2008**, *25*, 1158–1174.
(4) Xiang, T.-X.; Anderson, B. D. A computer simulation of functional group contributions to free energy in water and a DPPC lipid bilayer. *Biophys. J.* **2002**, *82*, 2052–2066.
(5) Norman, K. E.; Nymeyer, H. Indole localization in lipid membranes revealed by molecular simulation. *Biophys. J.* **2006**, *91*, 2046–2054.
(6) Klauda, J. B.; Kucerka, N.; Brooks, B. R.; Pastor, R. W.; Nagle, J. F. Simulation-based methods for interpreting X-ray data from lipid bilayers. *Biophys. J.* **2006**, *90*, 2796–2807.
(7) Bastug, T.; Patra, S. M.; Kuyucak, S. Molecular dynamics simulations of gramicidin A in a lipid bilayer: From structure-function relations to force fields. *Chem. Phys. Lipids* **2006**, *141*, 197–204.
(8) Warren, D. B.; Chalmers, D. K.; Hutchison, K.; Dang, W.; Pouton, C. W. Molecular dynamics simulations of spontaneous bile salt aggregation. *Colloids Surf., A* **2006**, *280*, 182–193.
(9) Chandrasekhar, I.; van Gunsteren, W. F. Sensitivity of molecular dynamics simulations of lipids to the size of the ester carbon. *Curr. Sci.* **2001**, *81*, 1325–1327.
(10) Sum, A. K.; Biddy, M. J.; de Pablo, J. J.; Tupy, M. J. Predictive molecular model for the thermodynamic and transport properties of triacylglycerols. *J. Phys. Chem. B* **2003**, *107*, 14443–14451.
(11) Small, D. M. *Handbook of Lipid Research Vol. 4, The Physical Chemistry of Lipids: From Alkanes to Phospholipids*; Plenum Press: New York, 1986; p 367.
(12) Larsson, K. *The Lipid Handbook*; Gunstone, F. D., Harwood, J. L., Padley, F. B., Eds.; Chapman and Hall: New York, 1986; p 337.
(13) Engelsen, S. B.; Brady, J. W.; Sherbon, J. W. Simulations of the aqueous solvation of trilaurin. *J. Agric. Food Chem.* **1994**, *42*, 2099–2107.
(14) van Buuren, A. R.; Tieleman, D. P.; de Vlieg, J.; Berendsen, H. J. C. Cosurfactants lower surface tension of the diglyceride/water interface: a molecular dynamics study. *Langmuir* **1996**, *12*, 2570–2579.
(15) Harmandaris, V. A.; Angelopoulou, D.; Mavrantzas, V. G.; Theodorou, D. N. Atomistic molecular dynamics simulation of diffusion in binary liquid *n*-alkane mixtures. *J. Chem. Phys.* **2002**, *116*, 7656–7665.
(16) Cui, S. T.; Cummings, P. T.; Cochran, H. D.; Moore, J. D.; Gupta, S. A. Nonequilibrium molecular dynamics simulation of the rheology of linear and branched alkanes. *Int. J. Thermophys.* **1998**, *19*, 449–459.
(17) van Buuren, A. R.; Berendsen, H. J. C. Molecular dynamics simulations of carbohydrate-based surfactants in surfactant/water/oil systems. *Langmuir* **1994**, *10*, 1703–1713.
(18) van Buuren, A. R.; Marrink, S. J.; Berendsen, H. J. C. A molecular dynamics study of the decane/water interface. *J. Phys. Chem.* **1993**, *97*, 9206–9212.

Scheme 1. Atom Labels of the Four Solutes Used in the Calculation of Decane → Tricaprylin Transfer Free Energies and Functional Group Contributions

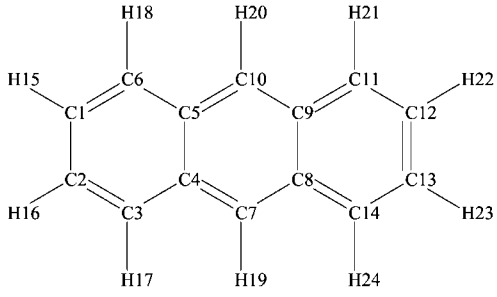

anthracene (ANT)

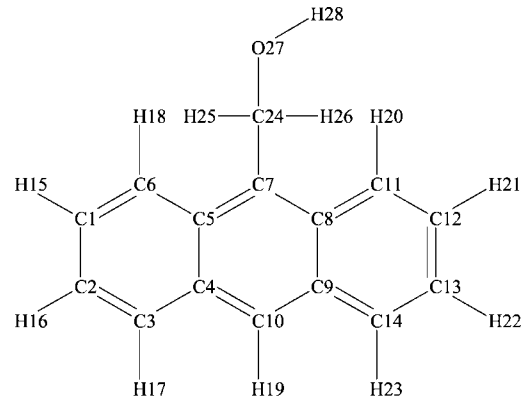

9-anthracene methanol (MET)

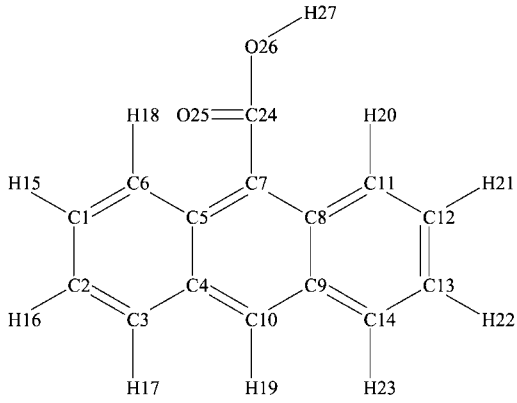

9-anthracene carboxylic acid (CAR)

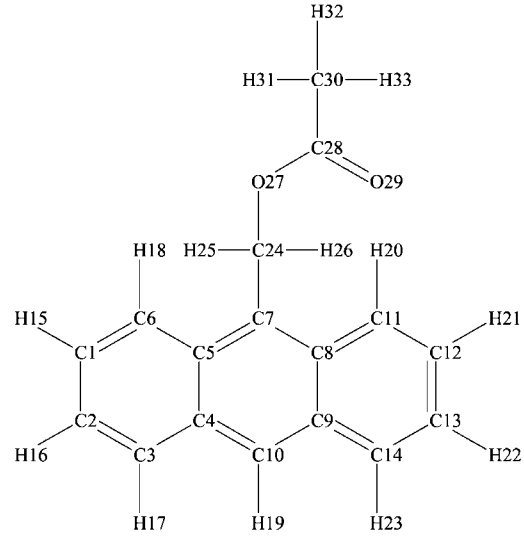

9-anthracenemethyl acetate (ACT)

Computation of functional group contributions to solvation free energies has also been reported using methods such as particle insertion, thermodynamic perturbation, and thermodynamic integration.[19−22] The combined thermodynamic perturbation and integration (TPI) approach is a popular route to calculate transfer free energies between solvents. The TPI approach is derived from first principle statistical thermodynamics and is exact as long as the mutation is performed extremely gradually.[23] The approach has been validated by a number of researchers.[19,24,25]

Methods

Molecular Dynamics Simulations. Two sets of simulations were conducted. In the first set, the thermodynamic perturbation and integration approach was employed to calculate polar functional group contributions to the free energies of transfer of a set of four 9-substituted anthracene analogues (Scheme 1) from *n*-decane to tricaprylin. A second simulation was performed in water-saturated tricaprylin

(19) Shirts, M. R.; Pitera, J. W.; Swope, W. C.; Pande, V. S. Extremely precise free energy calculations of amino acid side chain analogs: Comparison of common molecular mechanics force fields for proteins. *J. Chem. Phys.* **2003**, *119*, 5740–5761.

(20) Xiang, T.-X.; Anderson, B. D. A computer simulation of functional group contributions to free energy in water and a DPPC lipid bilayer. *Biophys. J.* **2002**, *82*, 2052–2066.

(21) Chipot, C.; Kollman, P. A.; Pearlman, D. A. Alternative approaches to potential of mean force calculations: free energy perturbation versus thermodynamic integration. Case study of some representative nonpolar interactions. *J. Comput. Chem.* **1996**, *17*, 1112–1131.

(22) Fukuda, M. Solubilities of small molecules in polyethylene evaluated by a test-particle-insertion method. *J. Chem. Phys.* **2000**, *112*, 478–486.

(23) Landau, L. D.; Lifshitz, E. M. *Statistical Physics*, 3rd ed.; Butterworth-Heinemann: Boston, 1980; Part 1, Vol. 5, pp 95−98.

(24) Hummer, G.; Szabo, A. Calculation of free-energy differences from computer simulations of initial and final states. *J. Chem. Phys.* **1996**, *105*, 2004–2010.

(25) Wescott, J. T.; Fisher, L. R.; Hanna, S. Use of thermodynamic integration to calculate the hydration free energies of *n*-alkanes. *J. Chem. Phys.* **2002**, *116*, 2361–2369.

Scheme 2. (a) Backbone Structure and Atom Labels of Tricaprylin (TRI)[a] and (b) Atom Labels of Benzamide (BEN)

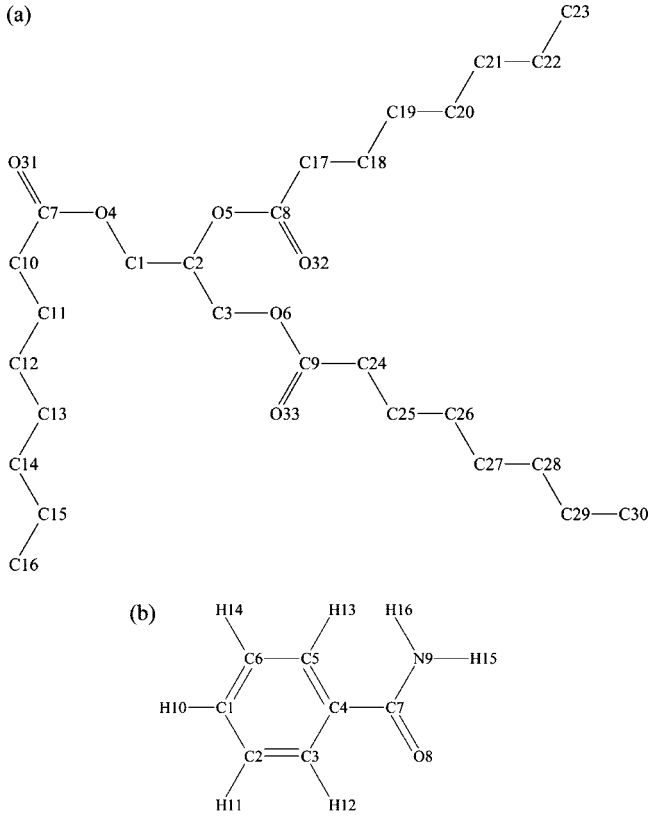

[a] The hydrogen atoms attached to atoms C1, C2, and C3 are (H34, H35), H36, and (H37, H38), respectively. The hydrogen atom labels in each arm are labeled serially from atom C10−C16, C17−C23, and C24−C30 as H39−H53, H54−H68, and H69−H83, respectively.

containing a single benzamide molecule (Scheme 2) to explore the organization of the triglyceride, the distribution of the dissolved water, and the local solvation shell surrounding the solute, benzamide.

Force Field and Molecular Models. All simulations were conducted using the SANDER program and the general amber force field (GAFF) in the AMBER 8 suite. Initial molecular assemblies were built using the xLeap module. Unscaled charges were calculated with the Antechamber program[26] in AMBER 8 using the AM1-BCC charge model. The charges from the AM1-BCC model closely replicate the charges from *ab initio* calculations at the level of HF/6-31G* basis set, which has been recommended for charge calculation in condensed matter simulations.[27,28] During the simulations, the charges of all atoms (solute and solvent) were scaled by multiplying the unscaled charges with a single scaling factor (γ) to account for the reduction of charges in the low polarization environment of the lipid mixtures. The structures and atom labels for all molecules (except *n*-decane) employed in this study are shown Schemes 1 and 2. (For reference purposes, the atom labeled as C7 is the 9-position using standard nomenclature.) The carbon atoms in *n*-decane (DEC) were serially labeled C1−C10 from one end to the other, and the hydrogen atoms were serially labeled as H11−H32 starting from C1−C10. The unscaled atomic charges for all the molecules (except water) are listed in Tables 1 and 2.

Simulation Details. In each simulation, first a cubic box was constructed with periodic boundary conditions in all three directions. The first set of simulations consisted of pure tricaprylin (121 molecules) and pure *n*-decane (244 molecules) along with a single 9-substituted anthracene molecule (Scheme 1). The simulation conducted in water-saturated tricaprylin consisted of 121 tricaprylin molecules, 1 benzamide, and 9 water molecules. After the box was constructed, the system was energy minimized with 1000 steps of steepest descent and conjugate gradient methods to remove bad contacts and a short, high pressure, constant temperature run was performed to bring the system density close to the final desired density. The systems were then equilibrated by molecular dynamics runs for ~20 ns with a time step of 1 fs under constant pressure (1 atm) and at a constant temperature of 37 °C for the first set of simulations and at 25 °C for the simulation in water-saturated tricaprylin in order to match the temperatures at which experimental data were available. These simulations were followed by 30 ns dynamic runs in which trajectory snapshots were recorded every 2−4 ps. At each time step, Newton's equations of motion were solved for all atoms with the Verlet leapfrog algorithm.[29] The lengths of all covalent bonds involving a hydrogen atom were held fixed with the SHAKE algorithm in AMBER 8. The tolerance for covalent bond length fluctuation involving a hydrogen atom was 0.00001. A cutoff distance of 10 Å was employed in the calculation of van der Waals interactions and electrostatic interactions using the particle mesh Ewald method.[30] The temperature was held constant by Langevin dynamics[31,32] with a collision frequency of 1.0. Constant pressure was maintained using the

(26) Wang, J.; Wang, W.; Kollman, P. A.; Case, D. A. Antechamber, an accessory software package for molecular mechanical calculations. *J. Comput. Chem.* **2005**, *25*, 1157–1174.
(27) Jakalian, A.; Bush, B. L.; Jack, D. B.; Bayly, C. I. Fast, efficient generation of high-quality atomic charges. AM1-BCC model: I. Method. *J. Comput. Chem.* **2000**, *21*, 132–146.
(28) Jakalian, A.; Jack, D. B.; Bayly, C. I. Fast, efficient generation of high-quality atomic charges. AM1-BCC model: II. Parameterization and Validation. *J. Comput. Chem.* **2002**, *23*, 1623–1641.
(29) Verlet, L. Computer experiments on classical fluids. I. Thermodynamical properties of Lennard-Jones molecules. *Phys. Rev.* **1967**, *159*, 98–103.
(30) Darden, T.; York, D.; Pedersen, L. Particle mesh Ewald - an Nlog(N) method for Ewald sums in large systems. *J. Chem. Phys.* **1993**, *98*, 10089–10092.
(31) Pastor, R. W.; Brooks, B. R.; Szabo, A. An analysis of the accuracy of Langevin and molecular dynamics algorithms. *Mol. Phys.* **1988**, *65*, 1409–1419.
(32) Loncharich, R. J.; Brooks, B. R.; Pastor, R. W. Langevin dynamics of peptides: The frictional dependence of isomerization rates of *N*-acetylalanyl-*N*′-methylamide. *Biopolymers* **1992**, *32*, 523–535.

Table 1. Unscaled Charges Obtained from the AM1-BCC Model for the Solute Molecules Anthracene (ANT), 9-Anthracene Carboxylic Acid (CAR), 9-Anthracene Methanol (MET), and 9-Anthracenemethyl Acetate (ACT)[a]

ANT		CAR		MET		ACT	
atom	charge	atom	charge	atom	charge	atom	charge
C10	−0.10666	O25	−0.54878	C3	−0.11987	C3	−0.11808
H19	0.1341	C24	0.65441	H17	0.13214	H17	0.1322
C4	−0.03358	O26	−0.6024	C2	−0.12541	C2	−0.12671
C3	−0.11767	H27	0.44238	H16	0.13325	H16	0.13306
H17	0.13202	C7	−0.10866	C1	−0.12444	C1	−0.12617
C2	−0.12664	C5	0.01818	H15	0.13408	H15	0.13228
H16	0.13217	C6	−0.12858	C6	−0.12039	C6	−0.1158
C1	−0.12666	H18	0.15463	H18	0.15024	H18	0.14025
H15	0.13215	C1	−0.11129	C5	−0.00909	C5	−0.00671
C6	−0.11769	H15	0.13765	C4	−0.04019	C4	−0.04056
H18	0.13202	C2	−0.12711	C10	−0.0957	C10	−0.09567
C5	−0.03358	H16	0.13604	H19	0.13524	H19	0.13514
C7	−0.10665	C3	−0.11494	C9	−0.04216	C9	−0.04147
H24	0.1341	H17	0.13431	C14	−0.11292	C14	−0.11568
C8	−0.03356	C4	−0.04934	H23	0.13301	C13	−0.12892
C9	−0.03361	C10	−0.07144	C13	−0.13084	C12	−−0.1208
C14	−0.11769	H19	0.13859	H22	0.13439	C11	−0.12574
H23	0.13202	C9	−0.05021	C12	−0.11896	H20	0.13652
C13	−0.12666	C8	0.02083	H21	0.13325	H21	0.13398
H22	0.13216	C11	−0.12386	C11	−0.13105	H22	0.13409
C12	−0.12664	H20	0.14686	H20	0.13177	H23	0.13254
H21	0.13217	C12	−0.11266	C8	−0.01384	C8	−0.00706
C11	−0.11767	H21	0.13657	C7	−0.11445	C7	−0.07205
H20	0.13202	C13	−0.12776	C24	0.16929	C24	0.17877
		H22	0.13605	H25	0.07234	H25	0.05556
		C14	−0.11389	H26	0.03344	H26	0.07083
		H23	0.13441	O27	−0.59749	O27	−0.43903
				H28	0.40434	C28	0.63178
						C30	−0.15034
						H31	0.07587
						H32	0.07726
						H33	0.0777
						O29	−0.54702

[a] These charges were multiplied by the scaling factor 0.79 during the simulations.

Berendsen method[33] with a relaxation time of 1.0 ps. The dielectric constant of the medium was set at 1.0 throughout all simulations. The ptraj program in Amber 8 was used for all analyses of molecular trajectories. The VMD program[34] was utilized for creating visual snapshots. All calculations were performed on a HP Superdome cluster and an XC cluster at the University of Kentucky, Lexington, KY.

Functional Group Contributions to the Free Energy of Transfer. Group contributions for various polar substituents (i.e., $-CH_2OH$, $-COOH$, and $-CH_2OCOCH_3$) at the 9-position of anthracene to the free energies of transfer of anthracene analogues from *n*-decane to pure tricaprylin were calculated using a combined thermodynamic perturbation and integration approach. The substituent values were found by subtracting the transfer free energy of anthracene from the transfer free energies for each 9-substituted anthracene.

In the calculation of the transfer free energy, the original solute structure was mutated to a reference solute in which the 9-substituents and charges on all atoms in the original solute were removed in both solvents, *n*-decane and tricaprylin. Starting with the well-equilibrated simulation box, the free energy calculations were performed in two steps. In the first step, the charges over the entire solute were nullified or removed. This step yields the free energy change associated with the "Coulombic forces", although the interdependence of the free energy from Coulombic and van der Waals forces does not allow for a clean separation.[19] In the second step, the substituent at the 9-position was gradually removed by perturbing the atoms in the functional group such that their radii were gradually reduced to zero (while all the other properties of the original atom type were retained).

(33) Berendsen, H. J. C.; Postma, J. P. M.; van Gunsteren, W. F.; Dinola, A.; Haak, J. R. Molecular dynamics with coupling to an external bath. *J. Chem. Phys.* **1984**, *81*, 3684–3690.

(34) Humphrey, W.; Dalke, A.; Schulten, K. VMD - Visual Molecular Dynamics. *J. Mol. Graphics* **1996**, *14*, 33–38.

Table 2. Unscaled Charges Obtained from the AM1-BCC Model for Tricaprylin (TRI), the Solute Benzamide (BEN), and *n*-Decane (DEC)[a]

TRI						BEN		DEC	
atom	charge	atom	charge	atom	charge	atom	charge	atom	charge
C16	−0.07807	C18	−0.07987	C25	−0.07825	C3	−0.07646	C10	−0.09255
H51	0.02843	C19	−0.07638	H71	0.0542	H12	0.15787	H30	0.03241
H52	0.02837	C20	−0.07405	H72	0.0485	C2	−0.13882	H31	0.03228
H53	0.02947	C21	−0.07514	C26	−0.07663	H11	0.13858	H32	0.03241
C15	−0.07703	C22	−0.07717	H73	0.03864	C1	−0.10779	C9	−0.08011
H49	0.03495	C23	−0.07785	H74	0.04035	H10	0.13519	H28	0.03834
H50	0.03699	H66	0.02918	C27	−0.0738	C6	−0.1401	H29	0.03833
C14	−0.07483	H67	0.02922	H75	0.04024	H14	0.1355	C8	−0.07929
H47	0.03953	H68	0.02927	H76	0.03802	C5	−0.10378	H26	0.03937
H48	0.03719	H64	0.03607	C28	−0.07512	H13	0.13233	H27	0.03937
C13	−0.07376	H65	0.0363	H77	0.03795	C4	−0.14165	C7	−0.07904
H45	0.03497	H62	0.03887	H78	0.03886	C7	0.67021	H24	0.0393
H46	0.04209	H63	0.03797	C29	−0.07681	N9	−0.67408	H25	0.03929
C12	−0.0755	H60	0.03777	H79	0.03701	H15	0.30693	C6	−0.07897
H43	0.04183	H61	0.04017	H80	0.03586	H16	0.3173	H22	0.0394
H44	0.03538	H58	0.0409	C30	−0.07796	O8	−0.61123	H23	0.0394
C11	−0.08439	H59	0.03756	H81	0.02935			C5	−0.07889
H41	0.03995	H56	0.04227	H82	0.02913			H20	0.03944
H42	0.07263	H57	0.05762	H83	0.0288			H21	0.03944
C10	−0.11095	H54	0.08511					C4	−0.07911
H39	0.0913	H55	0.08315					H18	0.03927
H40	0.0813	O32	−0.52204					H19	0.03927
C7	0.63024	H36	0.06091					C3	−0.07923
O31	−0.59106	C3	0.16387					H16	0.0394
O4	−0.399	H37	0.06681					H17	0.03941
C1	0.12842	H38	0.07246					C2	−0.08014
H34	0.0783	O6	−0.38975					H14	0.03831
H35	0.06362	C9	0.6134					H15	0.03829
C2	0.14448	O33	−0.58695					C1	−0.09251
O5	−0.42194	C24	−0.11426					H11	0.03243
C8	0.6331	H69	0.08552					H12	0.03227
C17	−0.14353	H70	0.08828					H13	0.03241

[a] These charges were multiplied by the scaling factor 0.79 during the simulations.

Scheme 3. Illustration of the Mutation Process for Converting a Given Solute to an Uncharged Reference Compound in the Calculation of the Transfer Free Energy

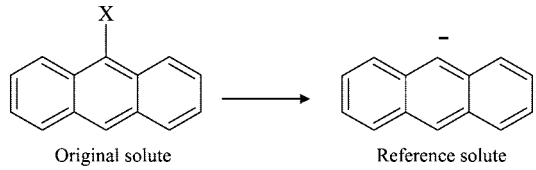

X = H (anthracene)
X = CH_2OH (9-anthracene methanol)
X = COOH (9-anthracene carboxylic acid)
X = CH_2OCOCH_3 (9-anthracenemethyl acetate)

This step may yield the free energy change attributable to van der Waals interactions. The sum of the free energy changes in these two steps yields the total free energy change in mutating the solute from one state to another. The overall mutation process and the structure of the reference solute are illustrated in Scheme 3.

The thermodynamic perturbation approach was used to calculate the derivative of the free energy with a mutation parameter, λ, as the solute was perturbed from the original molecule ($\lambda = 0$) to the final state ($\lambda = 1$). The free energy to mutate the solute from its original form RX to R (without the substituent, X) in a given solvent, tricaprylin or *n*-decane, was obtained by integration:

$$\Delta G^{RX\rightarrow R} = \int_0^1 \frac{\partial G}{\partial \lambda}\, d\lambda = \int_0^1 \left\langle \frac{\partial H(\lambda)}{\partial \lambda} \right\rangle_\lambda d\lambda \qquad (1)$$

Here, $H(\lambda)$ is the system Hamiltonian at the coupling parameter λ. The free energy to grow a hydrogen at the 9-position, $\Delta G^{R\rightarrow RH}$, which is the negative of $\Delta G^{RX\rightarrow R}$ when X = H at the 9-position (anthracene), is added to the mutation free energies for the three solutes. This yields the free energy to mutate the three anthracene-based solutes (containing the functional groups) to anthracene in a given solvent:

$$\Delta G^{RX\rightarrow RH} = \Delta G^{RX\rightarrow R} + \Delta G^{R\rightarrow RH} \qquad (2)$$

Finally, the free energy to mutate the original solute to anthracene in the two solvents decane (d) and tricaprylin (t) is subtracted to get the contribution of the functional group X to the free energy to transfer:

$$\Delta\Delta G^{X} = \Delta G_{d}^{RX\rightarrow RH} - \Delta G_{t}^{RX\rightarrow RH} \quad (3)$$

The removal of charges was accomplished with a step size of $d\lambda = 0.2$ while $d\lambda = 0.05$ for the van der Waals portion of the calculations. The $d\lambda$ value chosen for removal of charges was larger because the $dG/d\lambda$ curve for this mutation is usually a straight line or a simple curve. However, for atom disappearance, the $dG/d\lambda$ curve is quite complex, and small $d\lambda$ values are necessary to ensure that the correct area under the curve is obtained. The Sander program in AMBER 8 was implemented for the perturbation calculations, using an input file with klambda = 1 and 6 for the Coulombic and van der Waals calculations, respectively. The trapezoidal rule was applied to calculate the areas under the curves. During the mutations, first a 50 ps equilibration run was performed at each λ value and then $dG/d\lambda$ values were collected and averaged over the next 200 ps with an interval of 0.1 ps.

Results

Properties of Simulated Solvents and Evidence for Equilibration. The final box sizes in the MD simulations were about $47 \times 47 \times 47$ Å^3 and $44 \times 44 \times 44$ Å^3 for pure tricaprylin and *n*-decane, respectively, more than sufficiently large to ensure the absence of interactions between images of solvent atoms or between opposite ends of the same solvent molecule. Shown in Figure 1 are the fluctuations in solvent densities during the first 25 ns of the equilibration stages. The absence of systematic changes in the densities suggests that the equilibration times were sufficiently long. The solvent densities obtained during the equilibration stages of the simulations at 37 °C were ~0.943 and 0.712 g/cc for tricaprylin and *n*-decane, respectively, in good agreement with their experimental values.[35,36]

Shown in Figure 2a is the mean square displacement of benzamide for the first 20 ns of simulation time. The displacement exceeded the largest dimension of benzamide, indicating that the simulation time was sufficient to allow benzamide to sample various regions of the solvent. The decay in the orientation autocorrelation function of the vector from atom H10 to H16 in benzamide versus simulation time, displayed in Figure 2b, is complete in 5 ns, indicating that the molecule has freely rotated.

Group Contributions to the Free Energy of Transfer from Decane to Tricaprylin. The combined thermodynamic perturbation and integration method for determining functional group contributions to the free energy of transfer of 9-substituted anthracene analogues from decane to tricaprylin involved calculation of the derivative of the free energy as a function of a mutation parameter, λ. Shown in Figure 3a,b are $dG/d\lambda$ curves for the mutation processes depicted in Scheme 3 for 9-anthracene carboxylic acid in tricaprylin and *n*-decane to illustrate the differences in the complexity of the curves during charge removal (Figure 3a) and during removal of atoms in the substituent at the 9-position of anthracene (Figure 3b). These complexity differences justify the choice of different $d\lambda$ values for the two steps.

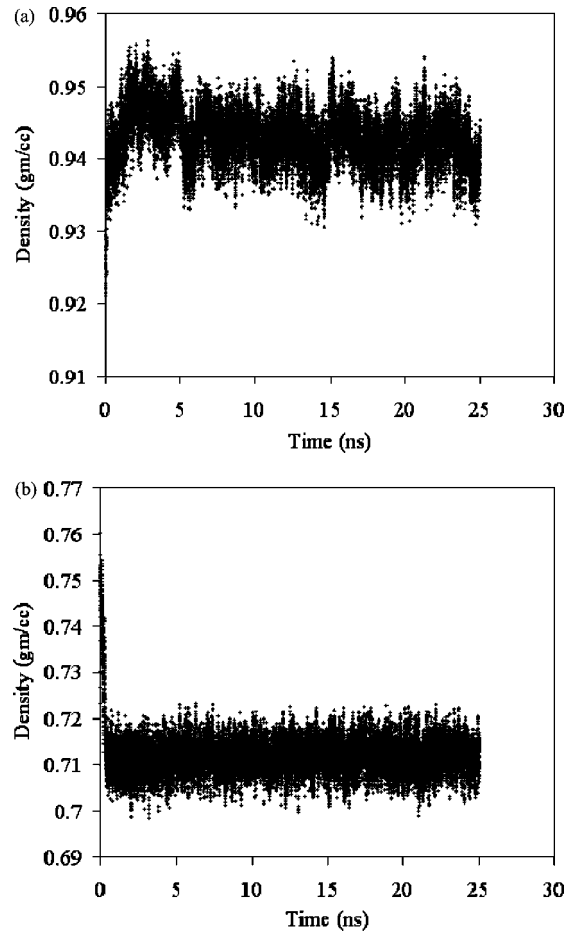

Figure 1. Fluctuations in density during a 30 ns equilibration run ($\gamma = 0.79$) in (a) pure tricaprylin and (b) pure *n*-decane with 9-anthracene carboxylic acid as the solute, at 37 °C.

As illustrated in Figure 3c, the average value for $dG/d\lambda$ converged rapidly in the simulation of 9-anthracene carboxylic acid in tricaprylin at a $\lambda = 0.5$ during the removal of atoms stage. The result shows that a data collection run time of 200 ps was sufficiently long to ensure that a correct average of $dG/d\lambda$ was obtained. In the initial simulations, some calculations were also performed with longer equilibration (100 vs 50 ps) and data collection times (400 vs 200 ps) but the results (not shown) were not significantly different from the results obtained at shorter times.

Summarized in Table 3 are the Coulombic and van der Waals contributions to the free energies of the four anthracene analogues in decane and tricaprylin generated from the two mutation processes (i.e., removal of charges (Coulombic component) and removal of all atoms in the 9-substituent (van der Waals component)) using various charge scaling factors. Average calculated group contributions to

(35) Gouw, T. H.; Vlugter, J. C. Physical properties of triglycerides. I. Density and refractive index. *Fette, Seifen, Anstrichm.* **1966**, *68*, 544–549.

(36) Landaverde-Cortes, D. C.; Iglesias-Silva, G. A.; Ramos-Estrada, M.; Hall, K. R. Densities and viscosities of MTBE + nonane or decane at $p = 0.1$ MPa from (273.15 to 363.15) K. *J. Chem. Eng. Data* **2008**, *53*, 288–292.

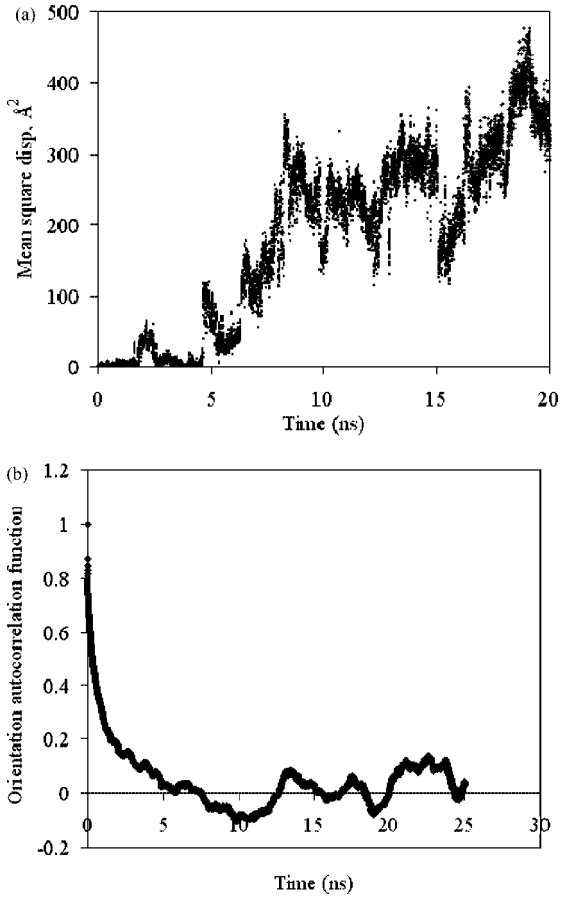

Figure 2. Relaxation characteristics of benzamide: (a) Mean square displacement of benzamide in wet tricaprylin. The large displacement indicates that the dynamics run was sufficiently long for equilibration. (b) Decay of the orientation autocorrelation function (OACF) for the end-to-end vector of benzamide (atoms H10−H16) in water-saturated tricaprylin. The OACF decays to zero in ~5 ns, indicating that benzamide rotation is rapid relative to the overall simulation times.

the free energies of transfer ($\Delta\Delta G^X$) (with standard deviations if applicable) are then listed for each scaling factor. Since a single simulation may not yield statistical information for the calculated free energies, three independent simulations were performed for $\gamma = 0.79$ using different starting structures, and the average $\Delta\Delta G^X$ values along with their standard deviations were calculated. Table 3 clearly shows that when charges were not scaled ($\gamma = 1$), the $\Delta\Delta G^X$ values for the three functional groups were dramatically overestimated as compared with the experimental values listed in the last column (obtained from ref 3). This could be because the atomic charges obtained with the AM1-BCC model are too high and represent the charges in a highly polar environment, such as in water.[27,28] Therefore, to account for the reduced polarization in a lipid environment, a charge scaling factor ($\gamma < 1$) was found to be necessary. Scaled atomic charges, q', on all solute and solvent atoms in both tricaprylin and *n*-decane were generated by multiplying the unscaled charges (q) obtained with the AM1-BCC model by the scaling factor, γ (i.e., $q' = \gamma q$). A scaling factor of $\gamma = 0.79$ was found by trial and error and repeated calculations to yield excellent agreement between the calculated and experimental values of $\Delta\Delta G^X$ for all three functional groups. Transfer free energies provide a good reference for determin-

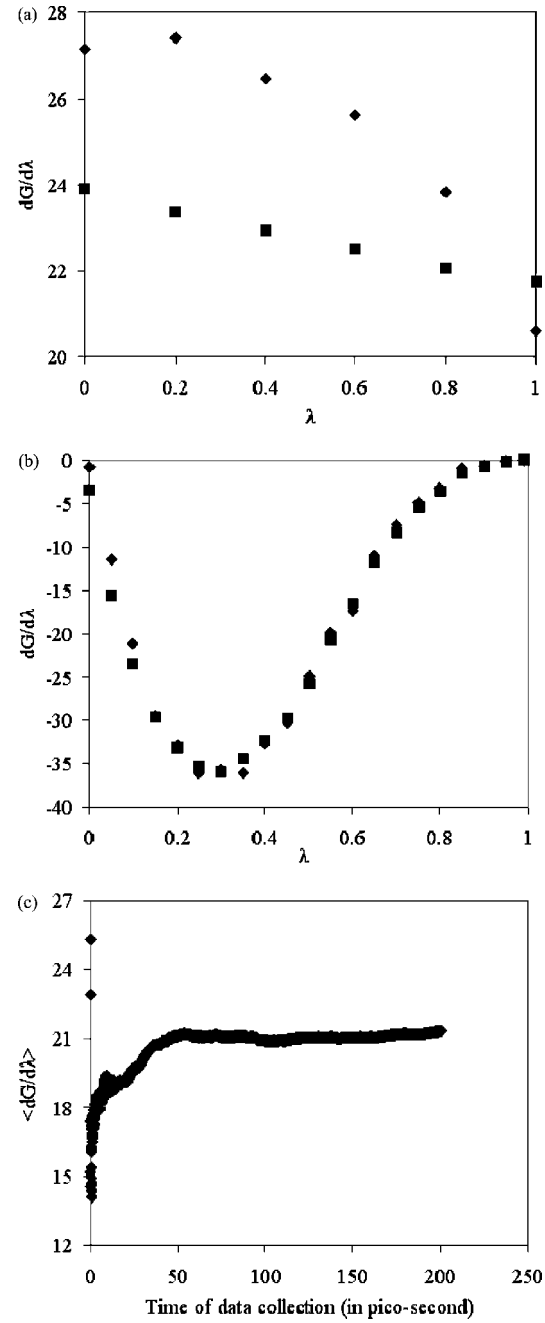

Figure 3. dG/dλ curves obtained in the mutation process for 9-anthracene carboxylic acid ($\gamma = 0.79$) described in Scheme 3: (a) curves obtained during the removal of charge [Coulombic part] in tricaprylin (◆) and *n*-decane (■); (b) curves obtained during the removal of 9-substituent atoms [van der Waals part] in tricapylin (◆) and *n*-decane (■); and (c) convergence of the average value of dG/dλ for the mutation of 9-anthracene carboxylic acid in tricaprylin, when the atoms are made to disappear after the removal of charges as a function of increasing data collection time.

Table 3. Group Contributions to the Decane → Tricaprylin Transfer Free Energies, $\Delta\Delta G^X$, for the Three Functional Groups at the 9-Position of Anthracene at 37°C[a]

			tricaprylin		*n*-decane			
solute	functional group of transfer (X)	charge scaling factor (γ)	Coulombic	van der Waals	Coulombic	van der Waals	average $\Delta\Delta G^X$	experimental $\Delta\Delta G^X$ [b]
ANT		1.0	4.92	−0.14	1.45	−0.2		
		0.84	2.02	−0.13	1.02	−0.19		
		0.79	1.9 (0.13)	−0.26(0.05)	0.92(0.02)	−0.19(0.02)		
CAR	COOH	1.0	44.64	−17.52	37.69	−18.35	−4.25	−2.94
	COOH	0.84	29.99	−17.88	25.86	−18.25	−3.43	−2.94
	COOH	0.79	25.83(0.37)	−17.59(0.48)	22.7 (0.06)	−18.24(0.13)	−2.85(0.55)	−2.94
MET	CH_2OH	1.0	8.01	−4.83	0.88	−4.73	−3.49	−1.5
	CH_2OH	0.84	3.77	−4.33	0.42	−4.83	−2.78	−1.5
	CH_2OH	0.79	2.37(0.59)	−4.2(0.22)	0.34(0.08)	−4.71(0.05)	−1.62(0.26)	−1.5
ACT	CH_2OCOCH_3	1.0						−0.54
	CH_2OCOCH_3	0.84	22.38	−4.46	20.32	−4.73	−1.27	−0.54
	CH_2OCOCH_3	0.79	19.7 (0.16)	−4.68(0.24)	17.88(0.07)	−4.49(0.05)	−0.7(0.17)	−0.54

[a] All energies are in kcal/mol. The penultimate column from the right shows the calculated average $\Delta\Delta G^X$ and standard deviations (if applicable). For the scaling factor of 0.79, three independent simulation runs were conducted ($n = 3$), whereas $n = 1$ for the scaling factors of 1.0 and 0.84. The last column on the right displays the previously published experimental results. The two columns under the headings "tricaprylin" and "*n*-decane" list the free energy changes during the mutation process in the two solvents for the removal of charges (Coulombic) and for the gradual removal of functional group atoms (van der Waals). As the scaling factor decreased for a given solute and solvent, the Coulombic contribution decreased and the van der Waals contribution remained almost fixed. [b] From ref 3.

ing the appropriate atomic charges because all thermodynamic functions can be derived from them.

Simulation of Water-Saturated Tricaprylin Containing Benzamide. A single molecule of benzamide was incorporated into a simulation box containing pure tricaprylin, and water molecules were added to match the experimentally determined water concentration in water-saturated tricaprylin.[37] Four such independent boxes were constructed to enable statistical analyses. The atomic charges were calculated with the AM1-BCC charge model as described before and reduced by a scaling factor ($\gamma = 0.79$) determined from the functional group contribution analyses. The concentration of water was deemed to be too low to significantly change the polarity of the solvent. As previous experimental[37] results for benzamide in tricaprylin were generated at 25 °C, these simulations were conducted at the same temperature.

Local Organization of Tricaprylin Molecules. The radial distribution function for the C2 atom (the middle atom in the glycerol backbone) of tricaprylin with the C2 atoms in neighboring tricaprylin molecules, shown in Figure 4, reveals a short peak at ∼5.2 Å, indicating that some local organization exists in liquid tricaprylin. This peak suggests some alignment of the glyceride backbone atoms and possibly also a segregation of the hydrophobic trigyceride alkyl chains. The possible existence of conformational preferences for the individual tricaprylin molecules was also examined. Two

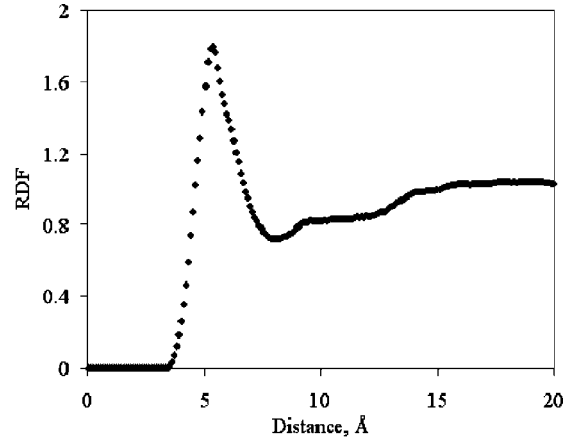

Figure 4. Radial distribution function of the central atom C2 in tricaprylin with the same atom in other tricaprylin molecules in the system. The small peak in the radial distribution function at ∼5.2 Å indicates that there is a weak ordering of polar and nonpolar domains in the liquid state. Pure tricaprylin may not be considered as a completely homogeneous liquid.

representative Ramachandran plots for the dihedral angles O5−C2−C1−O4 (α) and O5−C2−C3−O6 (β) on the glycerol backbone in tricaprylin are shown in Figure 5. The representative plots illustrate the conformational preferences of the three arms of different tricaprylin molecules. Different plots observed for different tricaprylin molecules may reflect different local structures in their vicinity. However, the plots show that each of the two outer arms of tricaprylin reside between (±) 50° and 100° from the middle arm. There is no population near 0°, probably because of steric hindrance

(37) Cao, Y.; Marra, M.; Anderson, B. D. Predictive relationships for the effects of triglyceride ester concentration and water uptake on solubility and partitioning of small molecules into lipid vehicles. *J. Pharm. Sci.* **2004**, *93*, 2768–2779.

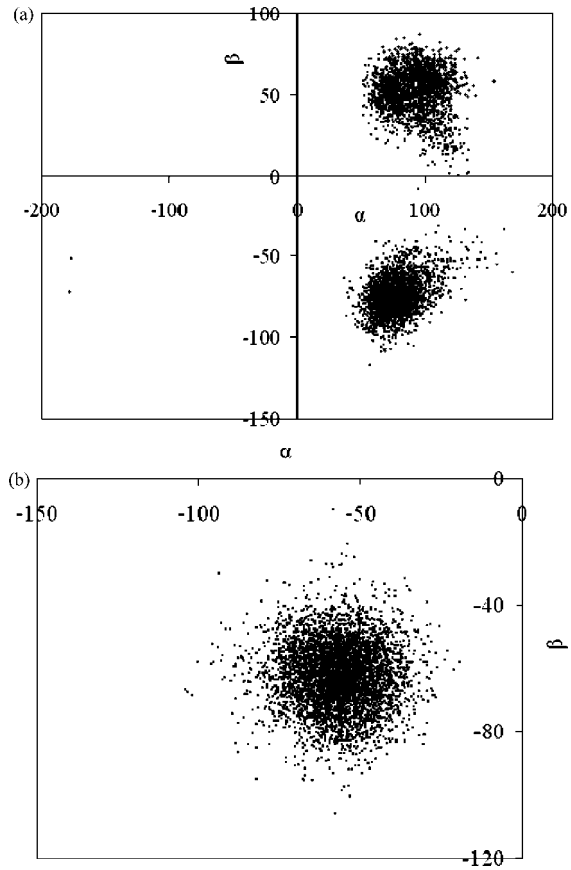

Figure 5. Ramachandran plots for the torsion angles O5−C2−C1−O4 (α) and O5−C2−C3−O6 (β) of tricaprylin. Two representative plots are shown for the different results that were observed in sampling the tricaprylin molecules. The plots show that each of the outer arms of tricaprylin reside between (±) 50° and 100° from the middle arm. There is no population near 0°, possibly because of steric hindrance with the middle arm.

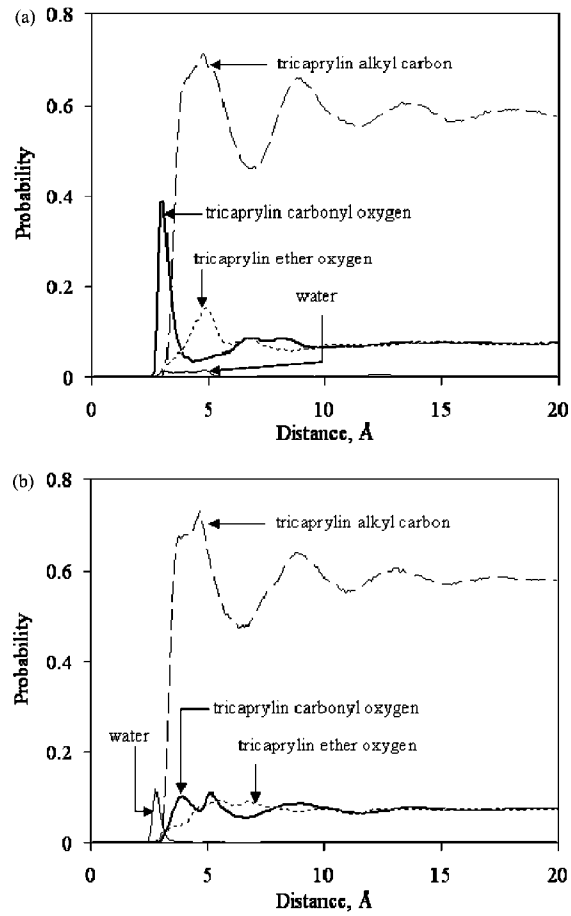

Figure 6. Absolute probabilities for finding a tricaprylin alkyl carbon [dashed line], carbonyl oxygen [thick solid line], ether oxygen [dotted line], and water [thin solid line] at various distances from the (a) amide nitrogen and (b) carbonyl oxygen (of benzamide). The ester carbonyl oxygen has a high probability of being close to the amide nitrogen and may engage in hydrogen-bonding with the amide group. There is a negligible presence of water in the neighborhood. There is also a substantially higher probability for the presence of water next to the carbonyl oxygen of benzamide as compared to the amide nitrogen. When water was located near benzamide, it generally hydrogen-bonded to the carbonyl oxygen while the amide nitrogen usually interacted with the tricaprylin ester carbonyl oxygen atoms.

with the middle arm. Ramachandran plots for various tricaprylin molecules (not shown) showed different signs for the two dihedral angles, indicating that there is no significant coupling between the relative motions of the two outer arms.

Distribution and Organization of Dissolved Water. Water-saturated tricaprylin at 25 °C has a relatively low concentration of water corresponding to just nine water molecules in the volume of solvent employed in the simulations. To investigate the structure of this dissolved water, the radial distribution function between water molecules (not shown) was examined. A very strong peak at ~2.8 Å was observed indicating that at least some of the water forms clusters in pure tricaprylin. However, such an analysis does not provide information on how many water molecules exist in clusters and how many are "free". For that purpose, a visual inspection of the water molecules was performed. It showed that, out of the nine water molecules, between three and seven molecules existed as "free" and the remaining molecules were present in one to two clusters containing two to three water molecules. Thus, on average, roughly half of the water molecules are "free" and the other half are in clusters.

Local Solvation Shell Surrounding Benzamide. To understand the molecular interactions that contribute to the overall free energy of benzamide in water-saturated tricaprylin, an examination of the local environment surrounding benzamide would be useful to ascertain the relative abundance of water, tricaprylin carbonyl oxygen atoms, ether oxygens, and tricaprylin alkyl chain carbon atoms. Shown in Figure 6a are the absolute probabilities for each of the above four different types of atoms as a function of distance from the amide nitrogen atom of benzamide, while the

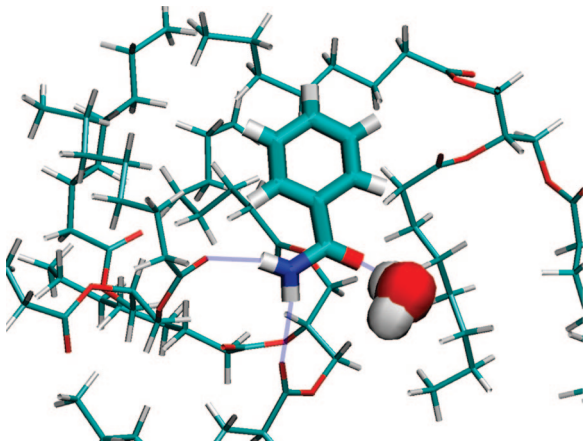

Figure 7. Snapshot from the simulation of water-saturated tricaprylin containing benzamide. The solute, benzamide, hydrogen bonds (shown by light blue bands) with polar groups on neighboring tricaprylin and water molecules.

absolute probabilities for the same four atoms as a function of distance from the carbonyl oxygen of benzamide are shown in Figure 6b. A maximum in the probability of locating an ester carbonyl oxygen atom within 3−4 Å of the benzamide nitrogen atom in Figure 6a suggests hydrogen-bonding between benzamide and a carbonyl oxygen atom in the triglyceride. The structure around the carbonyl oxygen atom of benzamide is quite different. As shown in Figure 6b, there is a substantially higher probability (∼11%) for a water molecule to be located within ∼3 Å of the carbonyl oxygen of benzamide, while tricaprylin carbonyl oxygen atoms are not in high concentration. Analysis of the dynamics trajectory and a visual inspection of the system revealed that if there is water molecule near benzamide, it was almost exclusively hydrogen-bonded to the carbonyl oxygen of benzamide, while the amide group hydrogen atoms were mostly hydrogen-bonded to tricaprylin carbonyl oxygen atoms. A representative snapshot of the simulation is shown in Figure 7, where the solute forms a 2−1−1 complex (2 = ester, 1 = water, 1 = benzamide). Hydrogen bonds are illustrated with light blue bands.

Discussion

Group Contributions to the Free Energy of Transfer from Decane to Tricaprylin. The reliable prediction of relative solubility of a given drug molecule in various lipid solvents solely from molecular dynamics simulations would be a valuable aid in drug formulation development. In the present study, functional group contributions to the free energy of transfer of a series of 9-substituted anthracene analogues from decane to tricaprylin were calculated by MD simulation and compared with experimental values previously published for the same solutes. The data summarized in Table 3 convincingly demonstrated that the calculated group contributions were much higher than the experimentally obtained values when the unscaled charges determined in AMBER 8 using the AM1-BCC charge model were employed in the simulations. Charges derived at the HF/6-31G* level are known to be more suitable for a polar environment (such as water)[27,28] because the theory overestimates the polarity of molecules by as much as 10−15% (over vacuum) in fortuitously accounting for solvent polarization. Therefore, one reason the group contributions to the transfer free energies may have been overestimated is because of higher (unscaled) atomic charges for the solute and solvent estimated in the simulations (the impact of atomic charge overestimates would be expected to be much larger in tricaprylin than in *n*-decane because tricaprylin has some polar groups but decane has none). In relatively nonpolar solvents such as those in this study, the atomic charges on both the solute and solvent evidently need to be corrected for the reduced polarization induced by the surrounding solvent environment. A number of studies[38,39] have shown that the atomic charges increase dramatically when a molecule is transferred from vacuum into a bulk solvent due to the increase in the polarization of the molecule from the surrounding medium (which varies with the hydrogen-bonding nature, polarity, and polarizability of the solvent). Marenich et al.[39] observed that solute atomic charges change monotonically with the solvent polarity. Gao et al.[40] found that the dipole moments calculated in the gas phase have a linear relationship with those in the aqueous phase. Thus, as a first approximation, it is reasonable to consider that the atomic charges on a solute may scale by a single factor depending on solvent polarity.[40,41] Scaling of atomic charges has also been implemented in a different context, for example, in approximately obtaining the HF/6-31G* charges from semiemperical wave functions[42,43] and to account for solvent screening effects in implicit solvation models.[44,45] Besler et al.[42] have found, for example, that the *ab initio* HF/6-31G* charges may be reasonably obtained by simply

(38) Tu, Y.; Laaksonen, A. Atomic charges in molecular mechanical force fields: A theoretical insight. *Phys. Rev. E.* **2001**, *64*, 026703.
(39) Marenich, A. V.; Olson, R. M.; Chamberlin, A. C.; Cramer, C. J.; Truhlar, D. G. Polarization effects in aqueous and nonaqueous solutions. *J. Chem. Theory Comput.* **2007**, *3*, 2055–2067.
(40) Gao, J.; Luque, F. J.; Orozco, M. Induced dipole moment and atomic charges based on average electrostatic potentials in aqueous solution. *J. Chem. Phys.* **1993**, *98*, 2975–2982.
(41) Kaminski, G. A.; Jorgensen, W. L. A quantum mechanical and molecular mechanical method based on CM1A charges: applications to solvent effects on organic equilibria and reactions. *J. Phys. Chem. B* **1998**, *102*, 1787–1796.
(42) Besler, B. H.; Merz, K. M.; Kollman, P. A. Atomic charges derived from semiempirical methods. *J. Comput. Chem.* **1990**, *11*, 431–439.
(43) Aleman, C.; Luque, F. J.; Orozco, M. Suitability of the PM3-derived molecular electrostatic potentials. *J. Comput. Chem.* **1993**, *14*, 799–808.
(44) Schwarzl, S. M.; Huang, D.; Smith, J. C.; Fischer, S. Nonuniform charge scaling (NUCS): A practical approximation of solvent electrostatic screening in proteins. *J. Comput. Chem.* **2005**, *26*, 1359–1371.
(45) Caldwell, J. W.; Kollman, P. A. Structure and properties of neat liquids using nonadditive molecular dynamics: water, methanol, and *N*-methylacetamide. *J. Phys. Chem.* **1995**, *99*, 6208–6219.

scaling charges linearly ($y = Mx$) from ESP charges of semiempirical methods such as MNDO. The authors found that this correlation is not perfect but sufficient to capture intermolecular interactions of various functional groups. Therefore, in this paper, we assumed that all charges on the solute and solvent could be scaled by a fixed factor ($\gamma < 1$) in relation to the charges derived at the HF/6-31G* level in order to account for the low polarity of bulk tricaprylin and *n*-decane. An alternative to this approximation would be to consider a different scaling factor for each solvent and for various functional groups[46] on the solute; however, that approach is naturally more complicated.

As shown in Table 3, as the scaling factor is reduced for a given solute and solvent, the Coulombic contribution obtained from the mutation process described previously decreases (because of the reduction in partial charges) but the van der Waals contribution is almost fixed. The independence or weak dependence of the van der Waals contribution on the scaling factor is expected, because once the charges on the functional group atoms are removed, they have no electrostatic interactions with the neighboring solvent atoms, and the van der Waals interactions are essentially the same (except for some minor structural changes in the solvent at different scaling factors). This observation is encouraging, because calculation of the van der Waals contribution is the most time-consuming part of the mutation process, and the results show that when the van der Waals contributions are calculated for one scaling factor, they are representative of the expected value at another similar scaling factor. The results also show that the Coulombic interactions, and hence the partial atomic charges, are extremely important in obtaining reliable transfer free energies. The functional group contributions to the free energy of solute transfer from decane to tricaprylin decreased (i.e., became more negative) with an increase in the hydrogen bond donating ability of the functional group (carboxylic acid > hydroxyl > ester), which is consistent with the fact that triglycerides possess complementary hydrogen bond acceptor groups. This supports the obvious expectation that specific interactions such as hydrogen-bonding may be one of the important considerations in determining relative solubility. Recent work in the application and comparison of different force fields for predicting solvation free energies in water has shown that AMBER in combination with the TPI approach does a good job in predicting free energies.[19] In the comparison of various charge models to calculate hydration free energies of small molecules, Mobley et al.[47] found that the AM1-BCC method for computing charges worked almost as well as the more expensive *ab initio* methods. In a recent work similar to the present study, Xiang and Anderson[20] adopted the TPI approach to study the transfer free energies of various functional groups from water into the interior regions of a lipid bilayer and illustrated that the transport barrier arises mainly because the interior region resembles a nonpolar hydrocarbon in terms of solvation interactions. GAFF was originally designed for simulations of organic molecules.[48,49] Its usefulness for aqueous lipid bilayer simulations was evaluated recently, by Jojart and Martinek,[50] Rosso and Gould,[51] and Siu et al.,[52] which showed that the results obtained from the simulations were reasonably good. However, there are limited data in the literature pertaining to the utility of AMBER for simulations in organic solvents.[53−55] The scaling factor of 0.79 obtained in this work, however, is consistent with the results of Xiang and Anderson[56] who demonstrated that charges in hydrophobic solvents such as carbon tetrachloride were as much as 20−25% lower than those in water.

The observation that the same scaling factor is applicable to both *n*-decane and tricaprylin (which have different polarities) naturally raises the question of what scaling factor can be expected in other solvents of different polarities. In this regard, it should first be noted that the upper limit for the scaling factor (1.0) is set by the charges derived in (highly polar) water. Our results in (highly hydrophobic) *n*-decane most likely identify a lower limit for the scaling factor (0.79). Presumably, different scaling factors would be necessary in other solvents and even then should be considered only as an approximate way to account for the variation in atomic charges resulting from polarization effects.

(46) Schwarzl, S. M.; Huang, D.; Smith, J. C.; Fischer, S. How well does charge reparameterisation account for solvent screening in molecular mechanics calculations? The example of myosin. *In Silico Biol.* **2003**, *3*, 187–196.

(47) Mobley, D. L.; Dumont, E.; Chodera, J. D.; Dill, K. A. Comparison of charge models for fixed-charge force fields: small-molecule hydration free energies in explicit solvent. *J. Phys. Chem. B* **2007**, *111*, 2242–2254.

(48) Wang, J.; Wolf, R. M.; Caldwell, J. W.; Kollman, P. A.; Case, D. A. Development and testing of a general amber force field. *J. Comput. Chem.* **2004**, *25*, 1157–1174.

(49) Case, D. A.; Cheatham, T. E.; Darden, T.; Gohlke, H.; Luo, R.; Merz, K. M.; Onufriev, A.; Simmerling, C.; Wang, B.; Woods, R. J. The amber biomolecular simulation programs. *J. Comput. Chem.* **2005**, *26*, 1668–1688.

(50) Jojart, B.; Martinek, T. A. Performance of the general amber force field in modeling aqueous POPC membrane bilayers. *J. Comput. Chem.* **2007**, *28*, 2051–2058.

(51) Rosso, L.; Gould, I. R. Structure and dynamics of phospholipid bilayers using recently developed general all-atom force fields. *J. Comput. Chem.* **2008**, *29*, 24–37.

(52) Siu, S. W. I.; Vacha, R.; Jungwirth, P.; Bockmann, R. A. Biomolecular simulations of membranes: Physical properties from different force fields. *J. Chem. Phys.* **2008**, *128*, 125103.

(53) Martin, M. G. Comparison of the AMBER, CHARMM, COMPASS, GROMOS, OPLS, TraPPE and UFF force fields for the prediction of vapor-liquid coexistence curves and liquid densities. *Fluid Phase Equilib.* **2006**, *248*, 50–55.

(54) Savest, N.; Oja, V.; Kaevand, T.; Lille, U. Interaction of Estonian kukersite with organic solvents: A volumetric swelling and molecular simulation study. *Fuel* **2007**, *86*, 17–21.

(55) Derreumaux, P.; Vergoten, G. Harmonic and molecular dynamics of *n*-octane. Comparison between the AMBER and SPASIBA force fields. *J. Mol. Struct.* **1993**, *295*, 233–244.

(56) Xiang, T.-X.; Anderson, B. D. Conformational structure, dynamics, and solvation energies of small alanine peptides in water and carbon tetrachloride. *J. Pharm. Sci.* **2006**, *95*, 1269–1287.

Simulations in Water-Saturated Tricaprylin. As discussed before, the temperature of the simulations in water-saturated tricaprylin (25 °C) was lower than that used in estimating the atomic charge scaling factor (37 °C). However, this difference is small enough that the scaling factor would not change significantly. This assertion is based on the observations that the dipole moments of bulk water or organic molecules have been found to change gradually with temperature.[57,58] Therefore, a 12 °C change in temperature is not expected to change the dipole moment of triglycerides significantly and, by extension, the atomic charges. That the same scaling factor would apply at 25 °C is also supported from the result that using a scaling factor of 0.79 the heat of vaporization of *n*-decane was calculated to be 51.32 kJ/mol (at 298 K), which matches with the experimental value of 51.4 kJ/mol.[59] The experimental heat of vaporization of tricaprylin could not be found in the literature.

Local Organization of Solvent Molecules in Liquid Tricaprylin. As discussed in the Introduction, some experimental and computer simulation studies had shown that pure triglyceride liquids are not completely structureless. Near the melting point, polar groups in pure triglyceride liquids may still aggregate in double layers as in their crystalline form, but the fatty acid chains are disordered.[11,12] With this background, one of the issues addressed in the current simulations was whether evidence for local solvent structure in tricaprylin could be obtained even though the simulation temperature employed (25 °C) is much higher than the melting point of tricaprylin (9 °C). Properly built and equilibrated simulation models should be able to reproduce the structure of these liquids in significant detail. Evidence for local structuring in tricaprylin was found, as indicated by the peak in Figure 4, that provided evidence for some alignment of the glyceride backbone atoms and possibly also a segregation of the hydrophobic trigyceride alkyl chains.

Distribution and Organization of Dissolved Water. As discussed previously, a strong peak at ~2.8 Å in the radial distribution function for water molecules in tricaprylin indicated the presence of hydrogen-bonded water−water dimers or larger aggregates in water-saturated tricaprylin. A visual inspection of snapshots from the simulations indicated that, on average, roughly half of the water molecules are "free" and the other half are in water clusters.

Xiang and Anderson observed that when water is present in poly(vinylpyrrolidone) (PVP) at low concentrations, it exists mainly in the form of free molecules.[60] The difference in the behavior of water in PVP and tricaprylin may be related to the numerous hydrogen-bonding sites available on the PVP chain. Water molecules may find a local PVP hydrogen-bonding site quite easily and may therefore have a reduced tendency to seek out other water molecules at low water concentrations. In tricaprylin, there is a substantially lower percentage of carbonyl oxygen atoms which can engage in hydrogen-bonding with the water molecules.

The state of dissolved water in triglycerides and other hydrocarbons has also been studied by Fourier transform infrared and near-infrared spectroscopy[61,62] where it has been found to exist in a variety of states from monomers to polymer clusters. In tristearin, the water distribution at 20 °C was found to be 24% monomeric, 16% dimeric, and 60% as trimers or higher polymers. Tricaprylin has not been studied experimentally, but the results for tristearin appear to be quite close to our MD simulation results.

Local Solvent Structure around Benzamide. Radial distribution functions shown previously in Figure 6 indicated that the nitrogen atom of benzamide interacts substantially with ester carbonyl oxygen atoms in tricaprylin most likely through hydrogen-bonding. The structure around the carbonyl oxygen atom of benzamide is different, with a substantially higher probability for the presence of water in the immediate vicinity.

The difference in the structure around the nitrogen and carbonyl oxygen atoms of benzamide may reflect the fact that the carbonyl oxygen can only interact with water via a hydrogen bond, whereas water oxygen atoms compete with the more abundant tricaprylin carbonyl oxygen atoms for the hydrogen donated by the amide group in benzamide. When both groups are hydrogen-bonded, the energy can be minimized. A visual and computational analysis of the four independent simulations on this system indicated that there is at most one water molecule around the benzamide at any given time. The simulations therefore suggest that the enhanced solubility of benzamide in wet tricaprylin versus dry tricaprylin observed by Cao et al.[37] is due to the influence of the dissolved water monomers. Although one to two small water clusters were found in the simulation box, the benzamide molecule typically was found to reside very far from them. The observations that benzamide is not solvated in/near the water clusters in tricaprylin or in wet tricaprylin/monocaprylin mixtures[63] gives new insight into the role of water in enhancing the solubility. In tricaprylin, where the water content is extremely low, the enhanced solubilization appears to originate from a direct interaction with monomeric water. In wet tricaprylin/monocaprylin mixtures,[63] where the

(57) Gubskaya, A. V.; Kusalik, P. G. The total molecular dipole moment for liquid water. *J. Chem. Phys.* **2002**, *117*, 5290–5302.
(58) Oriani, R. A.; Smyth, C. P. Dipole moment and restricted rotation in some chlorinated hydrocarbons. *J. Chem. Phys.* **1949**, *17*, 1174–1178.
(59) Dean, J. A. *Lange's Handbook of Chemistry*, 15th ed.; McGraw-Hill Inc.: New York, 1999; pp 6.58.
(60) Xiang, T.-X.; Anderson, B. D. Distribution and effect of water content on molecular mobility in poly(vinylpyrrolidone) glasses: A molecular dynamics simulation. *Pharm. Res.* **2005**, *22*, 1205–1220.
(61) Kurashige, J.; Takaoka, K.; Takasago, M.; Taru, Y.; Kobayashi, K. State of dissolved water in triglycerides as determined by Fourier transform infrared and near infrared spectroscopy. *J. Jpn. Oil Chem. Soc.* **1991**, *40*, 549–553.
(62) Takaoka, K.; Kobayashi, K.; Takahashi, M.; Sone, M. Analysis of the state of dissolved water in saturated, unsaturated, and aromatic hydrocarbons by FTIR spectroscopy and thermal stability of dissolved water. *Sekiyu Gakkaishi* **1999**, *42*, 93–100.
(63) Rane, S. S.; Anderson, B. D. Unpublished results.

water content is extremely large, changes in lipid organization induced by water appear to play an important role. Both factors may in turn influence the kind of complexes the solute can form with the solvent resulting in changes in solubility.

Occasionally, both hydrogens of the amide group of benzamide were found to engage in hydrogen-bonding with the carbonyl oxygen atoms of the tricaprylin molecules. From the standpoint of complex formation, it is desirable to investigate whether the two hydrogen atoms form bonds with the same tricaprylin molecule or different tricaprylin molecules and whether there is any pattern resulting from the structures of the molecules. For that purpose, the average distance between the three carbonyl oxygen atoms of the tricaprylin molecules was calculated from the trajectory data. The distances obtained are O31−O32 ∼ O32−O33 ∼ 5 Å and O31−O33 ∼ 6.5 Å. Thus, the distance between any two carbonyl oxygen atoms on the same tricaprylin molecule are large enough that the benzamide cannot form two hydrogen bonds with a single tricaprylin molecule. It is much more probable and easier for the amide hydrogen to form two hydrogen bonds with two different tricaprylin molecules.

Conclusions

Molecular dynamics simulations were conducted with the AMBER 8 general amber force field (GAFF) to explore the structural properties of triglycerides, and a combined thermodynamic perturbation and integration method was validated for the calculation of polar group contributions to the transfer free energies of 9-substituted anthracene analogues from *n*-decane to tricaprylin. Unscaled charges were obtained with the AM1-BCC charge model which closely reproduces charges that would be obtained by the application of the HF/6-31G* basis set. A scaling factor was then applied for evaluating the atomic charges of all molecules in low water content tricaprylin liquids. With this method, an atomic charge scaling factor of 0.79 was necessary to obtain functional group contributions that agreed with experiments in nonpolar lipids.

The simulations showed that pure tricaprylin liquids have some residual structure similar to the bilayer stacking of polar and hydrophobic domains in its crystalline state, but much weaker. The two outer arms of the tricaprylin molecule were oriented about ±50°−100° from the middle arm, and there was no significant coupling in their movement. The distance between the three carbonyl oxygen atoms of tricaprylin was large enough that the solute benzamide could not form more than one hydrogen bond with the same tricaprylin molecule. Whenever the two amide hydrogen atoms of benzamide formed two hydrogen bonds with the carbonyl oxygen of tricaprylin, it was with two different tricaprylin molecules. The water present in water-saturated tricaprylin was somewhat equally divided into "free" monomers and clusters of two to three molecules. In another paper,[63] the atomic charge scaling factor determined here has been employed to conduct MD simulations of triglyceride/monoglyceride/water w/o microemulsions to investigate their structural features and solute localization sites which may provide insights into solubility relationships in these systems.

Abbreviations Used

ANT, anthracene; CAR, 9-anthracene carboxylic acid; MET, 9-anthracene methanol; ACT, 9-anthracenemethyl acetate; TRI, tricaprylin; DEC, *n*-decane; BEN, benzamide.

Acknowledgment. S.S.R would like to thank the UK Supercomputer center for providing computer resources and support for conducting these simulations. The authors would also like to thank Pfizer Inc. for financial support of this project.

MP8000606